AIChE

Migration and Sedimentation of Spherical Particles in a Yield Stress Fluid Flowing in a Horizontal Cylindrical Pipe

Othmane Merkak, Laurent Jossic, and Albert Magnin
Laboratoire de Rhéologie, Domaine Universitaire, B.P. 53, 38041 Grenoble, Cedex 9, France, and
Institut National Polytechnique de Grenoble, Université Joseph Fourier Grenoble 1, CNRS, UMR 5520, France

DOI 10.1002/aic.11852
Published online July 28, 2009 in Wiley InterScience (www.interscience.wiley.com).

*This study looks at the dynamics of a particle suspended in a viscoplastic fluid, flowing in a horizontal circular cylindrical pipe. Inertia effects are negligible in comparison with viscous effects and plastic effects. The suspensions are highly stabilized and at rest the spheres cannot settle under gravity alone. The results of Merkak et al. (*AIChE J. *2008;54:1129–1138) are extended, taking into consideration both particles of the same density or denser than the fluid and pipe-to-particle diameter ratios of 8 or 56. New migration phenomena in the sheared zone are thus evidenced when buoyancy forces are nil. In the case of particles denser than the fluid, it is shown how the spheres settle by bypassing the plug-flow zone. A map showing the stability of flowing suspensions could, thus, be drawn.* © 2009 American Institute of Chemical Engineers *AIChE J,* 55: 2515–2525, 2009

Keywords: rheology, transport, complex fluids, fluid mechanics, multiphase flow

Introduction

Flows of suspensions often generate structuring phenomena that modify the initially random distribution of the particles and produce local variations in concentration. These phenomena have been discussed in numerous publications concerning suspensions of spherical solid particles flowing in cylindrical pipes. The fluids considered in these studies are mainly those with a Newtonian,[1–4] shear-thinning,[5] or viscoelastic[5] behavior.

Very little work has been carried out concerning suspensions in viscoplastic fluids. Jossic et al.[6] observed the migration of spherical solid particles toward the upper part of a cylindrical pipe in the case of a viscoplastic fluid in which the spheres were less dense than the fluid. Recently, Merkak et al.[7] performed an in-depth study of the dynamics of an isolated particle suspended in a viscoplastic velocity field and of the same density as the fluid.

This work showed that the dynamics of a particle suspended in a viscoplastic fluid flowing in a cylindrical pipe is a function of its position in the pipe. These results were obtained in cases where wall effects are very strong, the diameter of the pipe d being eight times that of the particles l. Hereinafter it will be assumed that $\lambda = d/l$. They observed that particles situated in the plug flow, mobile rigid zone, close to the centre line of the pipe had a translational motion. The second type of movement was both rotational and translational, affecting particles situated entirely or partly within the sheared zone. No migration of the particles was recorded. Indeed, with $\lambda = 8$, the sheared zone is smaller or of the same order of magnitude as the diameter of the particles, Figure 1. In this situation the migration phenomenon, if it exists, can only occur over very large timescales.

The purpose of this study is to examine two important new situations. The work is, therefore, divided into two parts. The first deals with suspensions in which the fluid and the particles have the same density. In the second part, the particles are denser than the fluid.

Correspondence concerning this article should be addressed to A. Magnin at magnin@ujf-grenoble.fr

The first part is an extension of the work of Merkak et al.,[7] with smaller particles such that $\lambda = 56$. This configuration is particularly interesting in that it produces sheared zones that are very thick in comparison with the diameter of the particles. In this configuration, it is therefore possible to examine the mechanisms of particle migration in the velocity field of the sheared zone close to the wall.

In the second part, the mechanisms of sedimentation and stability of flowing suspensions will be considered for two populations of spheres such that $\lambda = 56$ and $\lambda = 8$.

The fluids used are model viscoplastic gels carefully characterized from the rheometric point of view. The particles used are rigid, spherical, and noncolloidal, with a virtually monodisperse grading. The suspensions are diluted in such a way that there are no collective effects. At rest, the particles are held in suspension by the gel and cannot settle under the effect of gravity alone. Several gel/particle combinations are used. The suspensions flow in a horizontal cylindrical pipe of length $L = 105\ d$. Throughout this study, the flows are laminar, with significant plastic effects.

The experimental set-up used in this study was designed and validated by Merkak et al.[7] The flow set-up is fitted with advanced measuring and display systems so that the particles can be carefully monitored during flow. The absence of any slip at the wall during capillary flow was checked.[7]

Theoretical Approach

The suspensions studied consist of noncolloidal rigid spheres dispersed in a gelled model fluid. The fluid is a viscoplastic gel whose rheological behavior obeys the Herschel Bulkley model:

$$\begin{cases} \underline{\underline{\tau}} = 2\left(K\sqrt{-4D_{\mathrm{II}}}^{n-1} + \frac{\tau_o}{\sqrt{-4D_{\mathrm{II}}}}\right)\underline{\underline{D}} & \text{if} \quad -\tau_{\mathrm{II}} > \tau_0^2 \\ \underline{\underline{D}} = 0 & \text{if} \quad -\tau_{\mathrm{II}} \le \tau_0^2 \end{cases} \tag{1}$$

with τ_0 being the yield stress, K the consistency, n the flow index, $\underline{\underline{D}}$ the rate of deformation tensor, $\dot{\gamma}$ the second invariant of the rate of deformation tensor, $\underline{\underline{\tau}}$ the stress tensor deviator, and τ_{II} the second invariant of the stress tensor deviator. However, it should be noted that the model fluid used in this study has an elastoviscoplastic behavior as shown by Piau[8] (see the section on Material and Rheometry).

The flow of a yield stress fluid in a cylindrical pipe produces a velocity profile made of a plug flow zone, a mobile rigid zone near the centre line, where the stresses are lower than the yield stress, and a sheared zone near the walls, where the stresses are greater than the yield stress, Figure 1. Appendix gives the velocity profile equations for a Herschel-Bulkley fluid in steady conditions. The radius of the plug zone or mobile rigid zone is referred to as r_s. The thickness of the sheared zone is designated δ with $\delta = R - r_s$ where R is the radius of the pipe.

From the similarity study of the flow of a suspension of solid spheres in a viscoplastic fluid in a cylindrical pipe we can deduce the following dimensionless numbers. These are used to identify the effects that govern the flow.

The Reynolds number represents the ratio of inertia effects to viscous effects:

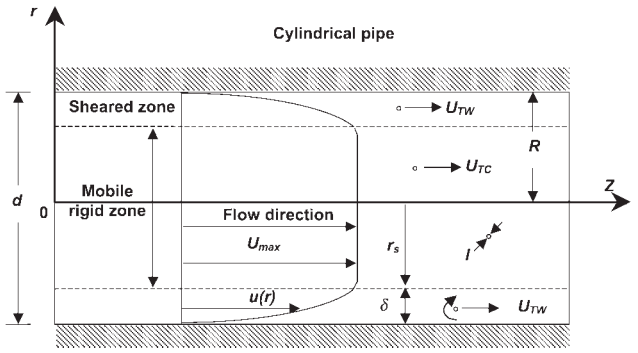

Figure 1. Velocity profile of a viscoplastic fluid flowing in a cylindrical pipe.

$$Re = \frac{\rho_f u^{2-n} d^n}{K} \tag{2}$$

ρ_f designates the density of the fluid and u the average velocity. In view of the velocities considered in this study, Re is between $\sim 10^{-7}$ and 0.04. Inertia effects are, therefore, negligible in comparison with viscous effects.

The Oldroyd number[9,10] represents the ratio of plastic forces to viscous forces

$$Od = \frac{\tau_0}{K\left(\frac{u}{d}\right)^n} \tag{3}$$

In the experimental conditions of this study, Od is between 0.5 and 13. Plastic effects are, therefore, significant in relation to viscous and inertia effects.

The particulate Reynolds and Oldroyd numbers, based on the diameter of the suspended particles, are written:

$$Re_p = Re.\lambda^{-n} \tag{4}$$

$$Od_p = Od.\lambda^{-n} \tag{5}$$

With $n \approx 0.4$, it can be shown that the particulate Reynolds numbers vary from 2×10^{-8} to 1.6×10^{-2}. The particulate Oldroyd numbers are between 0.1 and 5.16. The Reynolds numbers, therefore, remain low while the Oldroyd numbers cover an intermediate range. Shear-thinning is characterized by the flow index n.

The ratio of plasticity effects to gravity effects for a given particle is represented by:

$$Y = \frac{\tau_o}{gl\Delta\rho} \tag{6}$$

where l and $\Delta\rho$ designate respectively the diameter of a sphere and the difference in density between the particles and the fluid. The lowest value of Y beyond which the object is immobile in a fluid at rest is referred to as the stability criterion, denoted Y_S. Several studies concerning the value of Y_S, Beris et al.,[11] Chhabra,[12] Atapattu et al.,[13] Beaulne and Mitsoulis,[14] Jossic and Magnin,[15] and Merkak et al.[16] have shown that Y_S is between 0.048 and 0.111. When $Y > Y_S$, an isolated sphere is immobile and cannot move under the effect

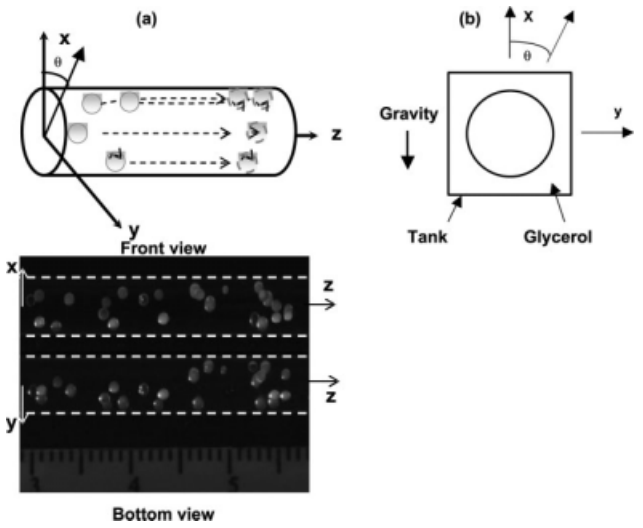

Figure 2. Three-dimensional particle flow upwards.

of gravity alone. When $Y < Y_S$, yield stress effects are weaker than gravity effects and the sphere can move. In this study, Y has values between 0.2 and 808. The suspensions are, therefore, stable at rest but with different degrees of intensity.

Another dimensionless number required to describe the flow is the ratio of the pipe diameter to that of the particles. Two sets of particles are used in this study with mean diameters of 100 and 690 μm. The pipe-to-particle dimension ratio is designated λ. The diameters of the pipe and particles thus give $\lambda = 56$ and $\lambda = 8$.

Experimental Set-Up

The experimental set-up used has already been described in detail.[7] It consists of a tank supplying a horizontal cylindrical pipe at constant velocity via a piston. The supply tank is made of transparent Plexiglass for viewing and checking that the preparation is homogeneous. The piston is driven by a thrust system via a controlled-speed motor. The pipe is made of treated transparent glass. It is $L = 580$-mm long and has a diameter $d = 5.5$ mm. Capillary flow was validated experimentally,[7] in particular to ensure that there was no slip at the wall.

The pressure in the pipe is measured with a pressure sensor supplied by Hirschmann, with an accuracy of the order of 0.2 mbar. The sensor is placed at the upstream end of the pipe at a distance of six diameters from the outlet from the tank. The pressure at the pipe outlet is atmospheric pressure.

Figure 2 shows the display principle. To correct the effects of curvature of the cylindrical pipe, it is immersed in a tank of pure glycerol, with the same refraction index as the pipe. The phenomena observed are displayed with a camera-mirror system. The Sony CCD camera is set perpendicular to the pipe to obtain a front view (plane containing the X and Z axes). To obtain a view from below (plane containing the Y and Z axes) a mirror inclined at 45° was used. The camera is connected to the mirror and can move along a rail to monitor the particles in the three dimensions of space along the flow. All the experiments were performed in an air-conditioned room at 23°C ± 1°C.

Table 1. Properties of Solid Particles

Materials	ρ (kg m^{-3})	Granulometry	
Glass	2,500	90–130	680–700
PMMA	1,190	90–130	680–700
Polystyrene	1,060	–	680–700

Material and Rheometry

The model suspensions used are made of a gelled fluid (water, polymer, and glucose) and spherical solid particles.

Three types of solid particles with different densities were used. The particles were made of glass, Plexiglas (PMMA), or polystyrene. Two populations of spherical particles were used, with grain size distributions from 90–130 to 680–700 μm. Table 1 summarizes the different properties of the solid particles studied. Some of the particles with grain-size distributions between 680 and 700 μm were marked with paint to measure their rotation speed.

The fluid is a model viscoplastic gel consisting of a mixture of water, Carbopol, and a solution of glucose. Carbopol 940 resin is a polymer manufactured by BF Goodrich—USA.[17,18] The water-glucose solution is prepared using pure glucose supplied by Nigay. S. A dissolved in demineralized water. Table 2 summarizes the properties of the fluids used.

After the two fluids have been mixed and then neutralized at pH 7, a transparent, viscoplastic aqueous gel is obtained. This is nonthixotropic with time-stable properties. The proportion of glucose is used to adjust the density and also increases the viscosity of the gel. The yield stress of the gel obtained in this way is adjusted by the concentration of Carbopol resin and control of the pH.

An aqueous solution of sodium azide NaN_3 prepared with a concentration of 20 g/l was used as bactericide. A dose of 1 ml of NaN_3 was added to each liter of glucose-Carbopol solution.

The yield stresses and rheological parameters of the fluids were carefully characterized by means of controlled strain rheometry. An ARG2 rheometer (TA Instruments) was used. The cone and plate have a rough surface state to prevent the sample from slipping on the surface of the tools.

The cone-plate cell is placed in a solvent trap to prevent evaporation from the sample. In addition, shear was

Table 2. Rheological Properties of Gels

Gels	Carbopol c_m (%)	Glucose c_m (%)	τ_0 (Pa)	K (Pa s^{-n})	n	ρ (kg m^{-3})	G' (Pa)	G'' (Pa)	pH
Gel 1	0.12	15	0.29	0.51	0.47	1050	8.15	0.78	6.8
Gel 2	0.2	15	10.4	3.02	0.46	1050	69.4	5	7.2
Gel 3	0.3	19	14.7	6.95	0.47	1170	120	9	7.1
Gel 4	0.4	15	56.6	21.7	0.33	1050	250	15	6.8

visualized by means of markers, to check the bulk deformation of the sample.[19,20]

Gelled fluids based on Carbopol behave as elastoviscoplastic materials.[8] To measure the elastic modulus below the yield stress, tests were performed under low-strain harmonic stresses. The elastic modulus G' is seen to be higher than the viscous modulus G''. The elastic modulus G' is constant depending on the strain. Table 2 gives the elastic modulus values for the different fluids. To determine the viscoplastic properties, high-strain tests were performed with shear rates ranging from 10^{-4} to 100 s^{-1}. Figure 3 shows the change in shear stress in steady conditions. A Herschel-Bulkley model, Eq. 1, was fitted for each fluid to determine the yield stress τ_0, consistency K, and shear-thinning index n.

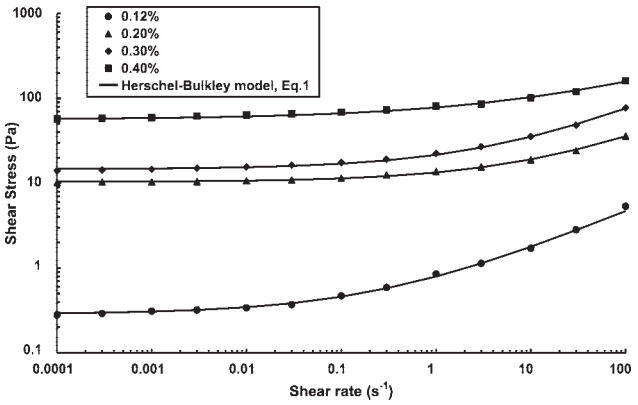

Figure 3. Experimental flow curves of carbopol-glucose gels.

Results and Discussion

Two situations were analyzed. In the first, the particles and gel have the same density. Gravity effects are, therefore, negligible. In the second, there is a difference in densities, with the spheres being denser than the fluid. Gravity effects may have a significant influence on the flow. It should be recalled that in all cases, at rest, the suspended particles do not settle as the fluid has a sufficient yield stress to counter gravity effects.

No gravity effects

Matas et al.[4] summarized the results found in the literature concerning suspensions in Newtonian fluids.[21–28] The main point to be borne in mind is that the migration of a particle in a flow is a nonlinear phenomenon. This nonlinearity may arise as a result of inertia, interactions between spheres or the non-Newtonian character of the fluid. Thus, when $Re = 0$, the Stokes equations, which are linear, predict that a solid particle cannot migrate laterally in a Newtonian fluid. With low Reynolds numbers, Segré and Silberberg[1] showed that there is an equilibrium position situated at $r = 0.62R$ in cases where the spheres have the same density as the fluid. This equilibrium position is the result of competition between a repulsion force due to the walls and a force due to the curvature of the shear field.

In the case of concentrated suspensions, particles migrate toward the low shear rate region of the flow.[29,30] Irreversible particle interactions in the presence of nonuniform shear gradients, concentrations, or viscosities generate migration phenomena under flow. This has been extensively studied,[31,32] particularly by nuclear magnetic resonance imaging.[33]

There are far fewer results for non-Newtonian fluids. In particular, those obtained by Karnis and Mason[34] and by Gauthier et al.[5] should be retained. The latter considered the phenomenon of lateral migration in the case of a pseudoplastic fluid. They showed that a rigid spherical particle migrates toward the wall. In the case of a viscoelastic fluid, they showed that the particles migrate toward the centre line of the pipe. In the case of yield stress suspending fluids, studies are still rare. Jossic and coworkers[6,35,36] observed new segregation and migration phenomena in laminar flow conditions at low Reynolds numbers, but without quantifying them.

According to Merkak et al.,[7] the dynamics of a particle suspended in a viscoplastic fluid flowing in a cylindrical pipe depends on its position in the pipe. With $\lambda = 8$, they observed the following:

displacement only by translation of particles situated in the central area of the pipe occupied by the mobile rigid zone or plug zone,

displacement by both rotation and translation in the case of particles situated partially or totally within the sheared zone close to the wall,

a fixed position in spite of flow for certain particles in contact with or very close to the wall.

We shall now consider the new case of smaller particles, $\lambda = 56$, where the thickness of the sheared zone, δ, may contain up to 12 particles. Let us, therefore, examine different cases depending on the positions of the particles in the pipe.

Particles in the Mobile Rigid Zone. As in the case where $\lambda = 8$, the particles situated in the mobile rigid zone move by translation, without any rotation or migration, when $\lambda = 56$. The translational speeds of particles in the plug zone are independent of their position in it.

Figure 4 represents the change in translational speed of particles situated in the plug zone depending on the Oldroyd number, for $\lambda = 8$ and $\lambda = 56$. The translational speed U_{TC} measured is made non dimensional by means of the maximum velocity of the gel without particles U_{max}. This figure also shows the change in average velocity u of the gel containing no particles made non dimensional by means of U_{max}. The variations are generally speaking similar for the two values of λ. With high Od numbers, the translational speed of the particle is equal to U_{max}, the velocity of the plug zone containing no particle. With very high Od values, the plug zone occupies almost the entire section. In addition, it can be seen that with the small particles, $\lambda = 56$, the regime with $u = U_{max}$ is reached at lower Oldroyd numbers. Indeed, the higher λ the less the flow is disturbed, and the particles tend to become tracers.

Calculating the ratio between the diameter of the plug zone $2r_s$, see Appendix, to the particle size gives:

$$\frac{r_s}{l} = \frac{\lambda}{2} - \frac{\delta}{l} \tag{7}$$

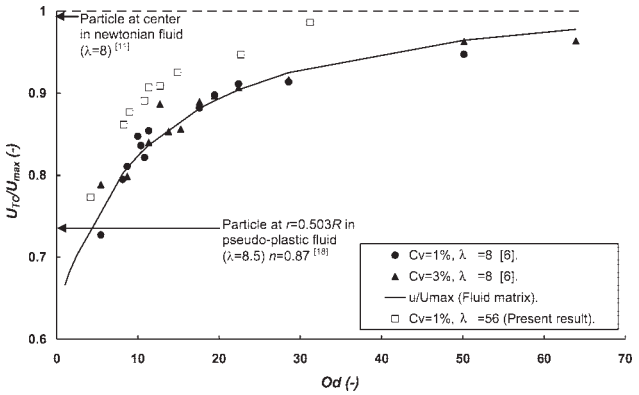

Figure 4. Change in translational speed depending on Oldroyd number.

In the case of the smallest particles, $\lambda = 56$, and the highest Od corresponding to $\delta/l \sim 14$, $r_s/l \sim 14$. Physically speaking, this means that a particle situated in the mobile rigid zone can never be considered to be isolated.

In the case of a Newtonian fluid, the formulae established by Greenstein and Happel[27] give $U_{TC}/U_{max} \approx 1$. This limiting case is illustrated in Figure 4. In the case where the fluid has a shear-thinning character, the experimental results of Gauthier et al.[5] give $U_{TC}/U_{max} \approx 0.76$ with a shear-thinning index $n = 0.87$ and $\lambda = 8.5$, for a sphere positioned at $r = 0.503R$. For the sake of comparison, this value is also plotted on Figure 4.

Particles in the Sheared Zone. Figure 5 shows an example of particles monitored during flow when $\lambda = 56$. The particle indicated by an arrow on Figure 5 was monitored as it moved. In Figure 5a, it is situated at a distance of about four times its diameter from the lower wall. It has moved by about 365 times its diameter from the time it entered the pipe. In Figure 5b, it has moved by about 400 times its diameter but it has also moved vertically by one time its diameter toward the central line of the pipe. The distance between the particle and the lower wall is then equal to five particle diameters. In Figures 5c, d, the particle continues to move along the flow and away from the lower wall of the pipe. It is situated, respectively, at 5 and 6 diameters from the lower wall in Figures 5c, d. In Figure 5e, the particle keeps its vertical position of about six times its diameter in relation to the lower wall. Figure 5f summarizes the trajectory that the particle has followed inside the sheared zone.

This type of migration was observed for several particles situated in the sheared zone and at different positions in the pipe, but not for all the particles situated in the sheared zone.

Merkak et al.[7] performed the same study for $\lambda = 8$, in the same pipe. No particle migration was recorded, as in this configuration the sheared zone was smaller or of the same order of magnitude as the diameter of the particles. The phenomenon of migration, if it exists, is very small scale. In contrast, when $\lambda = 56$, the particles are able to move in the sheared zone during flow.

Figure 6 represents the flow of a suspension of particles in the flow field of a viscoplastic fluid. The particles situated in the zone rigid move by translation without any radial migration or sedimentation.

The particles situated in the sheared zone move by rotation, which could be observed but not measured with the experimental set-up used, and by translation. No sedimentation of these particles was observed, simply their radial migration. This migration takes place in the sheared zone. The particles never enter the plug flow zone. The solid particles move toward the zone with the lowest shear rate. They, therefore, migrate toward the zone with a low shear rate in the direction of the plug zone. An equilibrium position of 0.46δ from the wall appears to be reached with Oldroyd numbers of $Od = 3.96$ ($n = 0.46$, $Y = 7.31$, $Re = 6.56.10^{-3}$, $\delta/l = 10.9$) and $Od = 5.45$ ($n = 0.46$, $Y = 7.31$, $Re = 2.26.10^{-3}$, $\delta/l = 8.88$).

Particles Near the Pipe Wall. As with $\lambda = 8$, the particles situated near the walls move by both rotation and translation without any migration when $\lambda = 56$. This case is summarized on Figure 6. This difference in comparison with the previous case arises perhaps from the combination of

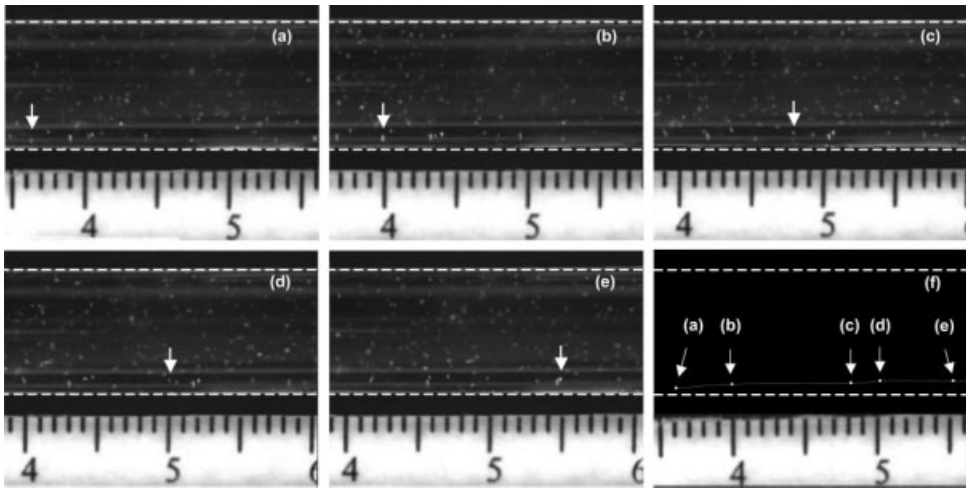

Figure 5. Migration of particles during flow of a suspension.

$C_v = 0.33\%$; $u = 4.05 \times 10^{-3}$ m s^{-1}; $Re = 6.56 \times 10^{-3}$; $Od = 3.96$; $\lambda = 56$; $\delta/l = 10.9$; $Y = 7.31$.

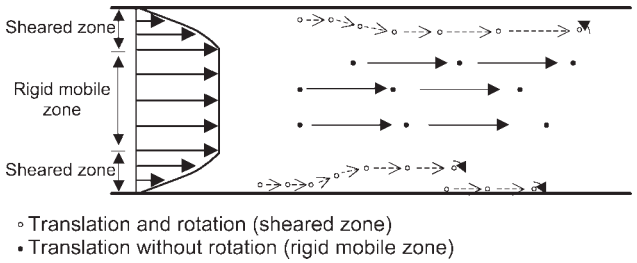

Figure 6. Schematic representation of particle displacement as a function of position in the pipe.

wall effects and plastic effects, the resultant of which prevents the particle from migrating. Merkak et al.[7] observed cases of no particle displacement at the wall when $\lambda = 8$. When $\lambda = 56$, no case of this type was observed.

Gravity effects: particles denser than the fluid

Dynamics of Sedimentation. The dynamics of particle sedimentation during flow in a cylindrical pipe was analyzed in this part of the study. Figure 7 represents the typical case of a suspension consisting of spherical solid glass particles, 690 μm in diameter, $\lambda = 8$, in a Carbopol-glucose gel with a concentration of 0.2% of Carbopol, Table 2. The difference in density between the solid particles and the fluid is 1450 kg/m^3. In this situation, $Y = 1.04 > Y_S$, and the particles are, therefore, stable when the suspension is at rest. Figure 7 shows two cases: when the particles are in the mobile rigid zone and when they are in the sheared zone. In each case, the particle's trajectory is monitored in three dimensions, Figure 2. The particles were marked with a black line to detect any possible rotation.

Particles in mobile rigid zone. Figures 7Ia–c show the displacement of a particle located in the mobile rigid zone. In all three sequences, the mark on the particle remains on the left side, even after a displacement equal to 20 times its diameter. This particle keeps the same position in the (X, Y) plane and follows a streamline parallel to the centre line of the pipe. It therefore moves with a translational motion, without any rotation or sedimentation.

Particles in sheared zone. Figure 7II shows the change in position of particle no. 2, situated in the sheared wall zone. Figure 7IIa shows that, in the (X, Z) plane, particle no. 2 is situated at three times its diameter from the upper wall of the pipe. During flow, between photos IIa and IIb, the particle has moved more than 37 times its diameter. It is then situated at 4 diameters from the upper wall of the pipe. Figure 7IIc shows that particle no. 2 is situated at seven times its diameter after moving more than 52 times its diameter. This particle, situated in the sheared zone, therefore settles as the suspension flows.

The particles were marked to visualize their rotations. In the case shown in Figure 7, the mark is situated on the upper part of the particle, Figure 7IIa. During flow, the mark moves toward the central part, Figure 7IIb and then the lower part, Figure 7IIc. The particle, therefore, moves by both rotation and translation in addition to settling toward the bottom of the pipe.

The particles situated in the mobile rigid zone move by translational motion without rotation and without sedimentation. The sedimentation mechanisms are located in the sheared zone part. The particles situated in the sheared zone settle during flow whereas they do not when the suspension is at rest.

Particles flowing at different velocities were monitored to determine the dynamics of sedimentation of a single particle. Figures 8 and 9 represent the trajectories during sedimentation in the XZ and YZ planes. Monitoring was performed at different Reynolds numbers. These figures show the position of the particle along the X and Y axes, adimensionalized by the radius of the pipe depending on the time adimensionalized by a characteristic time: the ratio between the length of the pipe and the mean flow velocity.

The settlement trajectories are curved. Three-dimensional monitoring of the particles shows that they never cross the mobile rigid zone. Sedimentation from the top of the pipe to

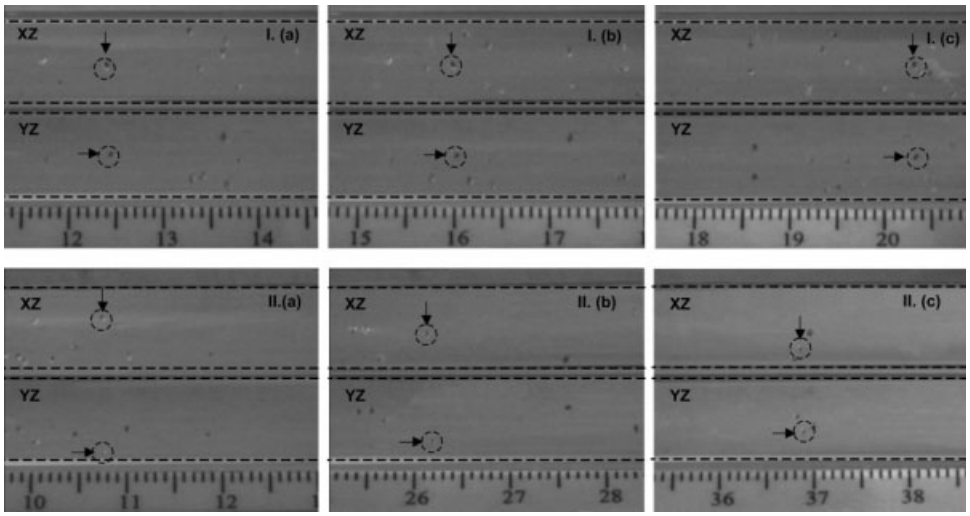

Figure 7. $C_v = 1\%$; $u = 4.05 \times 10^{-3}$ m s^{-1}; $Re = 1.78 \times 10^{-2}$; $Od = 10.82$; $\lambda = 8$; $\delta/l = 1.56$; $Y = 1.04$.

I: Particle located in the mobile rigid zone. II: Particle located in the sheared zone.

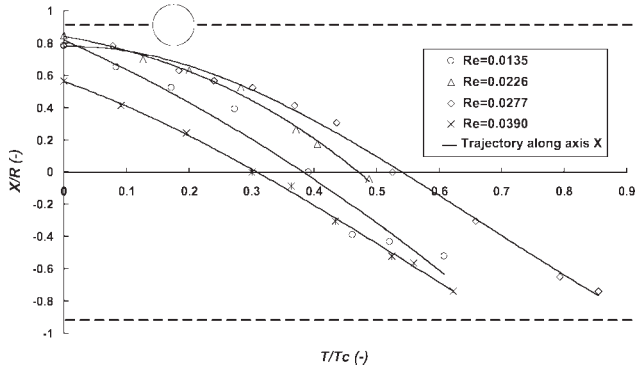

Figure 8. Change in dimensionless position of particles during sedimentation in *XZ* plane.

the bottom takes place in the sheared zone. The particle bypasses the plug flow zone until it reaches its final position at the bottom of the pipe.

The diagram shown in Figure 10 summarizes the different mechanisms of particle sedimentation during flow of the suspension in a cylindrical pipe. To summarize, two cases are observed:

Displacement by translational motion alone without any sedimentation of the particles situated in the plug flow zone. In this mobile rigid zone, the shear gradient is zero and therefore no torque is exerted on the particle. The particle is trapped in this zone, and moves by translation. In addition, as $Y > Y_s$, the particle does not settle.

Displacement by both rotation and translation with sedimentation of the particles situated in the sheared flow zone. By following an almost helical trajectory, the particles settle while remaining in the sheared zone and bypassing the plug flow zone, as far as the equilibrium position at the bottom of the pipe. In the sheared zone, the shear rates field exerts a torque and associated force on the particle, causing it to rotate and translate in the same way as a particle of the same density as the fluid, that is to say without gravity effects, as demonstrated by Merkak et al.[7] However, in the case studied, gravity exerts a vertical force and thus produces a sedimentation velocity toward the bottom of the pipe.

Stability of Suspensions. Figures 7 and 11 illustrate the different typical cases observed during the flow of suspensions in a cylindrical pipe. Two types of monitoring were

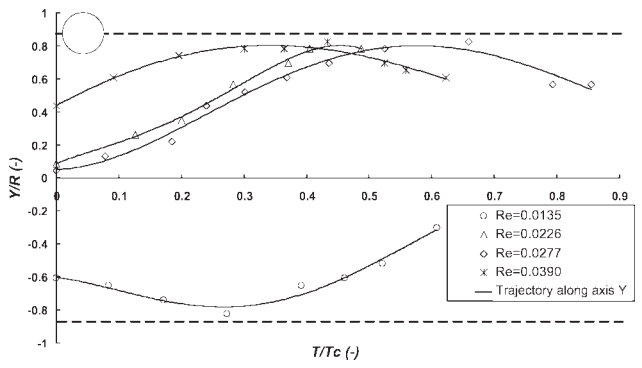

Figure 9. Change in dimensionless position of particles during sedimentation in *YZ* plane.

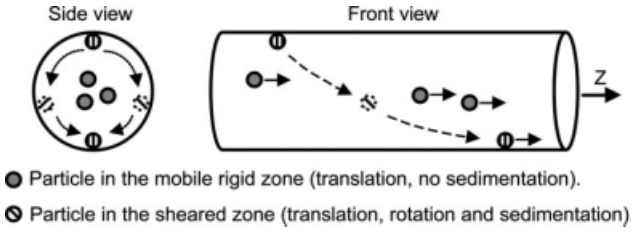

Figure 10. Schematic representation of the sedimentation of particles denser than the fluid.

used. The first is Lagrangian monitoring, used in the case of large particles measuring 690 μm in diameter. The second is Eulerian monitoring, used in the case of suspensions of particles measuring 100 μm in diameter. Figure 7, which was discussed in the previous section, shows the sedimentation of 690 μm particles during flow when $Y = 1.04 > Y_s$.

Figure 11 represents several cases. Figure 11I shows a suspension that remains stable during flow when $\lambda = 8$. When $Y = 808$, the suspension is, therefore, extremely stable. The particles do not settle, between the entry and exit of the pipe, Figures 11Ia, b. Figure 11II shows the case of a suspension such that $\lambda = 56$ and $Y = 11.3$. There is no difference in local concentrations between the entry and the exit of the pipe, Figure 11IIa, b. No significant particle sedimentation was observed on the flow timescale, in spite of a relatively high ratio between the size of the sheared zone and the size of the particles, $\delta/l = 14$.

Figure 11III also shows the case of a suspension such that $\lambda = 56$ but with $Y = 2.11$. The ratio of the size of the sheared zone to the size of the particles is $\delta/l = 18$. In this case, there is a distinct difference in the distribution of concentrations between the start and end of the pipe, Figures 11IIIa, b. At the pipe entrance, the particle distribution is homogeneous and random. Toward the pipe outlet, a significant proportion of the particles are situated at the bottom of the pipe, Figure 11IIIb. Even though $Y = 2.11$ is higher than the critical value Y_S, particle sedimentation has occurred in the pipe. Flow has destabilized the suspension and made it heterogeneous.

On the basis of these observations, it was possible to plot a stability diagram for all the experimental conditions. The flows all have low Reynolds numbers ($3 \times 10^{-7} < Re < 3 \times 10^{-2}$), in the case of all the suspensions used. Figure 12 shows the different Reynolds numbers involved, for the different values of Y. Figure 13 shows the different Oldroyd numbers, ($0.5 < Od < 15$) involved, for different values of Y.

Figure 14 represents a stability diagram in the XZ plane depending on the ratio of the size of the sheared zone to the particle size, δ/l. An interval of δ/l ranging from 0.3 to 30 was covered. The value of the stability criterion Y_S corresponding to an isolated sphere in an infinite medium in a fluid at rest was also placed on this figure. It shows that the values of Y for which the suspensions remain stable during flow are distinctly higher than Y_S, in the parameter range studied. The suspensions are stable for values of Y of the order of 3 to 4. For the fluid used in this study, a higher yield stress is, therefore, needed to stabilize a flowing suspension than one that is at rest.

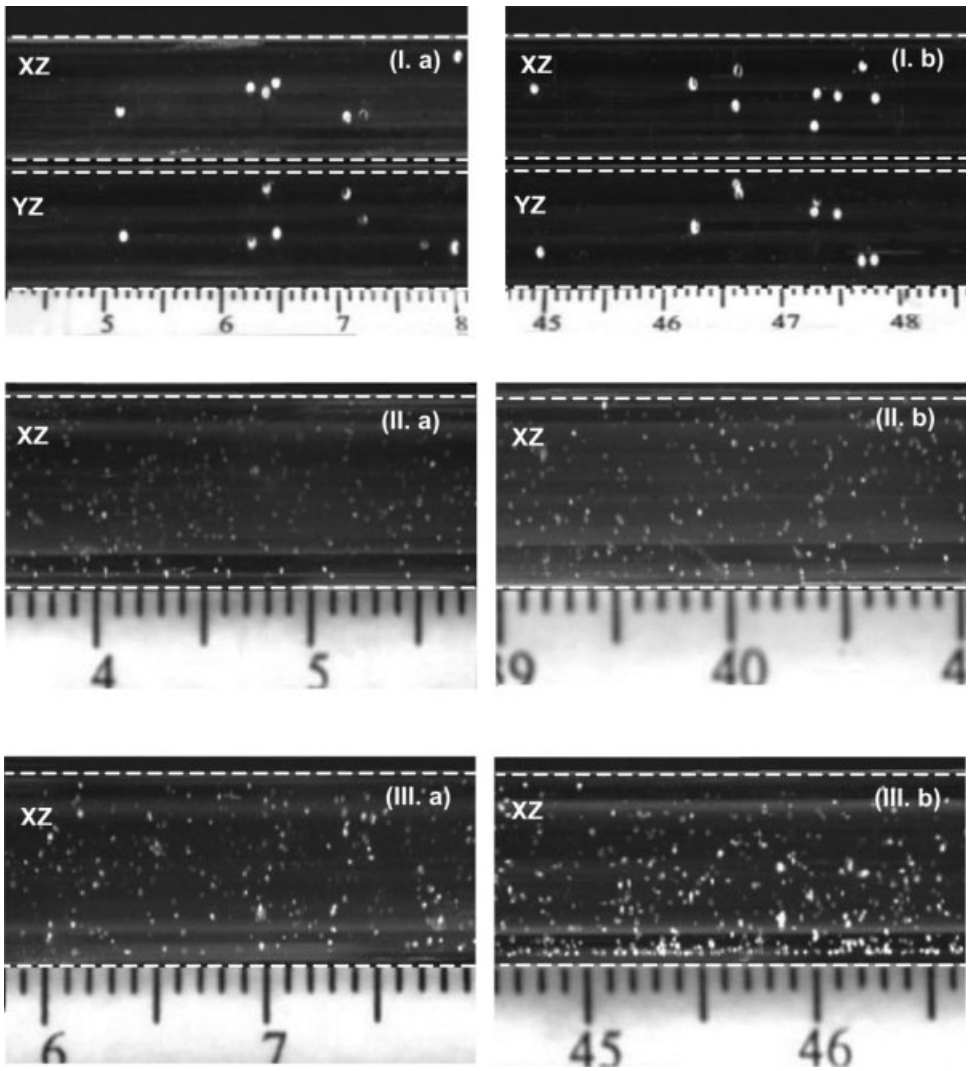

Figure 11. Particle sedimentation and stability during flow in a cylindrical pipe.

I: Stable suspension. $C_v = 1\%$; $Re = 2.4 \times 10^{-3}$; $Od = 2.37$; $\lambda = 8$; $\delta/l = 1.72$; $Y = 808$. II: Stable suspension. $C_v = 0.33\%$; $Re = 2.8 \times 10^{-3}$; $Od = 2.57$; $\lambda = 56$; $\delta/l = 14$; $Y = 11.3$. III: Unstable suspension. $C_v = 0.33\%$; $Re = 3.3 \times 10^{-3}$; $Od = 1.4$; $\lambda = 56$; $\delta/l = 18$; $Y = 2.11$.

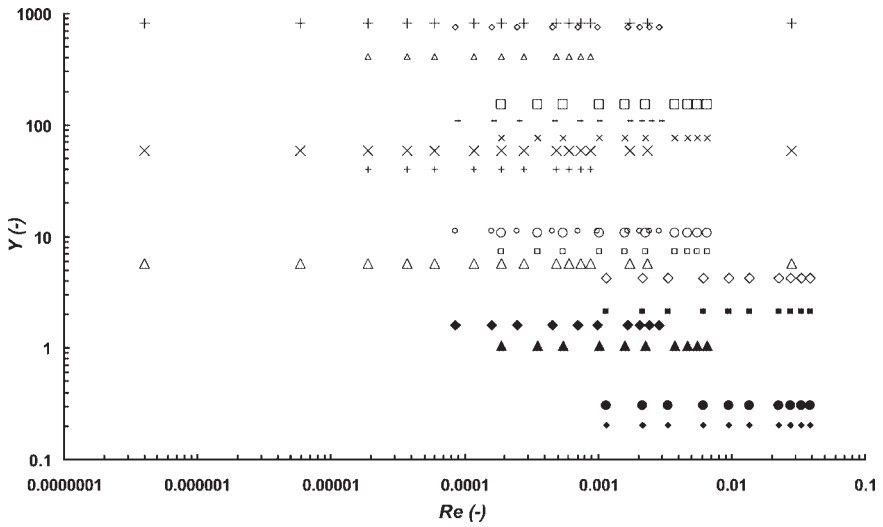

Figure 12. Stability criteria as a function of Reynolds number (see Table 3).

Table 3. Stability Criteria as a Function of Reynolds Number, Oldroyd Number, and Thickness of Sheared Zone

Y	Polystyrene		PMMA		Glass	
Carbopol	100 μm	690 μm	100 μm	690 μm	100 μm	690 μm
0.12 (%)	–	4.22 (◇)	2.11 (■)	0.302 (●)	0.204 (◆)	–
0.20 (%)	–	151 (□)	75.7 (×)	10.8 (○)	7.31 (□)	1.04 (▲)
0.30 (%)	–	–	750 (◇)	107 (−)	11.3 (○)	1.61 (◆)
0.40 (%)	–	808 (+)	412 (△)	58.9 (×)	39.8 (+)	5.68 (△)

It is possible to propose a change in the stability criterion outside the range studied experimentally. In the case of very low Reynolds numbers and very high Oldroyd numbers where the ratio of the size of the sheared zone to the size of the particle, δ/l, tends toward zero, the stability criterion Y_S should tend toward the value of the stability criterion of an isolated particle in a gelled fluid at rest, indicated on Figure 14 by isolated particle.[14] Strictly speaking, account should be taken of the effect of confinement at rest.

In the other extreme case, the sheared zone tends to occupy the entire pipe and the value of Y to stabilize this flowing suspension tends toward infinity as the particle always settles unless the spheres have the same density as the fluid.

Conclusion

This study demonstrated the mechanisms of migration and sedimentation of particles suspended in viscoplastic fluids, flowing in a cylindrical pipe. The flows considered have low Reynolds numbers and intermediate to high Oldroyd numbers. Plastic effects are predominant in comparison with viscous and inertia effects. The suspensions used are stabilized at rest. The solid particles are rigid with an almost monodisperse grain-size distribution. Two ratios between the diameter of the particle and that of the pipe were used, $\lambda = 8$ and $\lambda = 56$.

Two cases were studied depending on the difference in density between the fluid and the suspended solid particles.

In the case where gravity effects are zero, particles situated in the plug zone do not migrate radially during flow. They move by translational motion without rotation. When $\lambda = 56$, the thickness of the sheared zone is of the order of several particle diameters. Migration of certain particles in the sheared zone was observed. These particles move toward zones with lower shear rates. The particles move with a translational speed and rotation speed toward an equilibrium position at 0.46δ from the wall, with the fluids used in the present study. Some of the particles, close to the wall, move by both rotation and translation without any visible migration.

In the case where the particles are denser than the fluid, gravity effects become significant. The mechanisms of sedimentation of these solid particles were demonstrated. The particles situated in the plug zone do not settle. Particle sedimentation during flow occurs in the sheared zone. The particles have a helical trajectory. They do not cross the plug flow zone but bypass it. They have a horizontal and vertical translational motion and rotational motion. A stability criterion was determined for solid particles suspended in a viscoplastic fluid flowing in a cylindrical pipe. In the field of study explored here, this stability criterion is of the order of 3. Above this value, a suspension of solid particles may flow without being destabilized. This value is higher than for a suspension at rest.

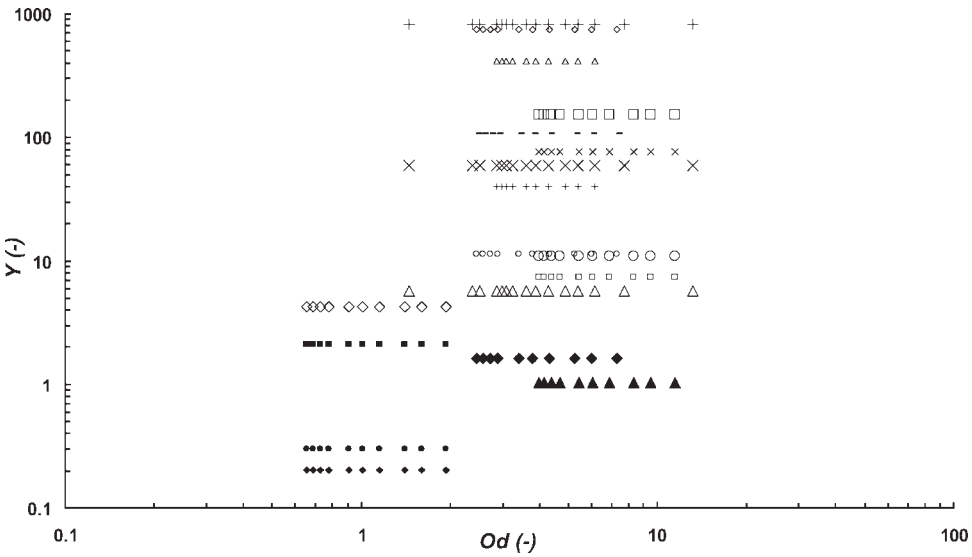

Figure 13. Stability criteria as a function of Oldroyd number (see Table 3).

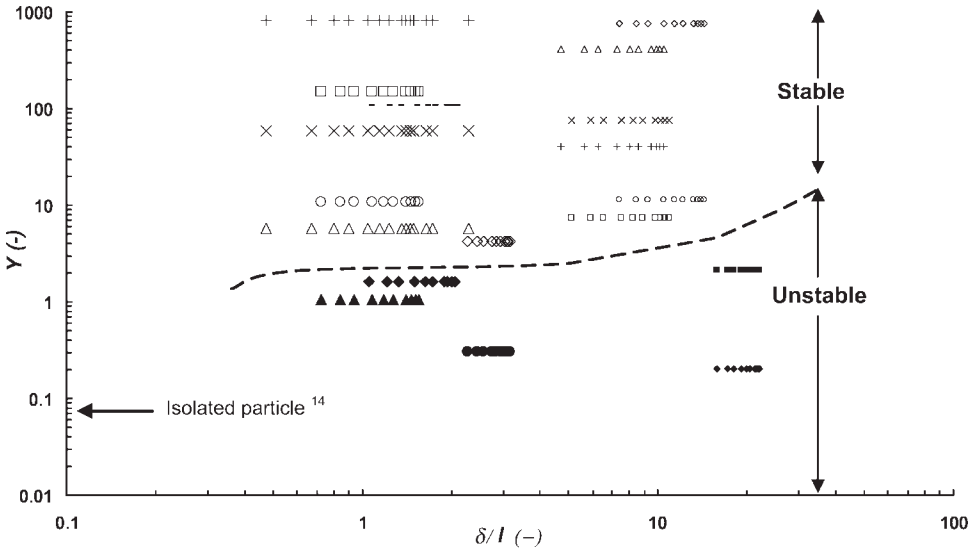

Figure 14. Stability criteria as a function of thickness of sheared zone (see Table 3).

These results are given for the experimental conditions of this study. The questions of sensitivity, detection, influence of observation time, and pipe length remain open. Nevertheless, the observations made here provide new basic knowledge on flows of suspensions in viscoplastic fluids. Thus, they open up prospects for future models. Theoretical and numerical modeling of the phenomena should provide additional help.

Acknowledgments

The authors thank Prof. Jean-Michel Piau for his helpful comments.

Notation

d = diameter of the pipe, m
g = gravity, m s^{-2}
G' = elastic modulus, Pa
G'' = viscous modulus, Pa
K = consistency, Pa s^n
l = diameter of the particles, m
L = length of the pipe, m
n = flow index
r_s = radius of the plug flow zone, m
R = radius of the pipe, m
U = velocity, m s^{-1}

Greek letters

τ = shear stress, Pa
τ_0 = yield stress, Pa
$\dot{\gamma}$ = shear rate, s^{-1}
γ = strain
ρ = density, kg m^{-3}
δ = thickness of the sheared zone, m

Dimensionless numbers

Re = Reynolds number
Re_p = particulate Reynolds number
Od = Oldroyd number
Od_p = particulate Oldroyd number
Y = ratio of yield stress to gravity effects
Y_S = stability criterion
$\lambda = d/l$ = ratio of pipe to particle diameters

Indices

C = center
P = particle
T = transfer
W = wall
max = maximum

Literature Cited

1. Segré G, Silberberg A. Behaviour of macroscopic rigid spheres in Poiseuille flow, Part 2: Experimental results and interpretation. *J Fluid Mech*. 1962;14:136–157.
2. Feng J, Hu HH, Joseph DD. Direct simulation of initial value problems for motion of solid bodies in a newtonian fluid, Part 1: Sedimentation. *J Fluid Mech*. 1994;95:271–301.
3. Matas JP, Morris JF, Guazzelli E. Transition to turbulence in particulate pipe flow. *Phys Rev Lett*. 2003;90.
4. Matas JP, Morris JF, Guazzelli E. Inertial migration of rigid spherical particles in Poiseuille flow. *J Fluid Mech*. 2004;515:171–195.
5. Gauthier F, Goldsmith HL, Mason SG. Particle motions in non-Newtonian media. II. Poiseuille flow. *Trans Soc Rheol*. 1971;15:297–330.
6. Jossic L, Briguet A, Magnin A. Segregation under flow of objects suspended in a yield stress fluid and NMR imaging visualisation. *Chem Eng Sci*. 2002;57:409–418.
7. Merkak O, Jossic L, Magnin A. Dynamics of the suspended particles in yield stress fluid matrix during its flow in the pipe. *AIChE J*. 2008;54:1129–1138.
8. Piau JM. Carbopol gels: elastoviscoplastic and slippery glasses made of individual swollen sponges: meso- and macroscopic properties, constitutive equations and scaling laws. *J Non-Newtonian Fluid Mech*. 2007;144:1–29.
9. Oldroyd JGT. A rational formulation of the equations of plastic flow for a Bingham solid. *Proc Cambridge Philos Soc*. 1947;43: 100–105.
10. Oldroyd JGT. Two-dimensional plastic flow of a Bingham solid. A boundary-layer theory for slow motion. *Proc Cambridge Philos Soc*. 1947;43:383–395.
11. Beris AN, Tsamopoulos JA, Armstrong RC, Brown RA. Creeping motion of a sphere through a Bingham plastic. *J Fluid Mech*. 1985;158:219–244.
12. Chhabra RP. *Bubbles, Drops and Particles in Non-Newtonian Fluids*. Boca Raton, FL: CRC Press, 1993.
13. Atapattu DD, Chhabra RP, Uhlherr PHT. Creeping motion in Herschel-Bulkley fluids: flow field and drag. *J Non-Newtonian Fluid Mech*. 1995;59:245–265.

14. Beaulne M, Mitsoulis E. Creeping motion of a sphere in tubes filled with Herschel-Bulkley fluids. *J Non-Newtonian Fluid Mech*. 1997;72:55–71.
15. Jossic L, Magnin A. Drag and stability of objects in a yield stress fluid. *AIChE J*. 2001;47:2666–2672.
16. Merkak O, Jossic L, Magnin A. Spheres and interactions between spheres moving at very low velocities in a yield stress fluid. *J Non-Newtonian Fluid Mech*. 2006;133:99–108.
17. B. F.Goodrich. *Carbopol Resins Handbook*. Cleveland, OH: B. F. Goodrich, 1997.
18. B. F.Goodrich. *Carbopol Resins Handbook*. Cleveland, OH: B. F. Goodrich, 1998.
19. Magnin A, Piau JM. Shear rheometry of fluids with a yield stress. *J Non-Newtonian Fluid Mech*. 1987;23:91–106.
20. Magnin A, Piau JM. Cone and plate rheometry of yield stress fluids. Study of an aqueous gel. *J Non-Newtonian Fluid Mech*. 1990;36:85–108.
21. Brenner H, Happel J. Slow viscous flow past a sphere in a cylindrical tube. *J Fluid Mech*. 1958;4:195–213.
22. Happel J, Brenner H. *Low Reynolds Number Hydrodynamics*. Prentice-Hall, The Hague: Martinus Nijhoff Publishers, 1965.
23. Goldsmith HL, Mason SG. The flow of suspensions through tubes. I. Single spheres, rods, and discs. *J Colloid Sci*. 1962;17:448–476.
24. Denson CD, Christiansen EB, Salt DL. Particle migration in shear fields. *AIChE J*. 1966;12:589–595.
25. Brenner H. Hydrodynamic resistance of particles at small Reynolds numbers. *Adv Chem Eng*. 1966;6:287–438.
26. Cox RG, Brenner H. The lateral migration of solid particle in Poiseuille flow. I. Theory. *Chem Eng Sci*. 1968;23:147–173.
27. Greenstein T, Happel J. Theoretical study of the slow motion of sphere and a fluid in a cylindrical tube. *J Fluid Mech*. 1968;34:705–710.
28. Cox RG, Mason SG. Suspended particles in fluid flow through tubes. *Annu Rev Fluid Mech*. 1971;3:291–316.
29. Gadala-Maria F, Acrivos A. Shear induced structure in a concentrated suspension of solid spheres. *J Rheol*. 1980;35:191–201.
30. Hampton RE, Mammoli A, Graham AL, Tetlow N, Altobeli SA. Migration of particles undergoing pressure driven flow in a circular conduit. *J Rheol*. 1997;41:621–640.
31. Leighton D, Acrivos A. The sheared induced migration of particles in concentrated suspensions. *J Fluid Mech*. 1997;275:155–199.
32. Philips RJ, Armstrong RC, Brown RA, Graham AL, Abott JR. A constitutive model for concentrated suspensions that accounts for shear-induced particle migration. *Phys Fluids A*. 1992;4:30–40.
33. Fukushima E. Nuclear magnetic resonance as a tool to study flow. *Annu Rev Fluid Mech*. 1999;31:95–123.
34. Karnis A, Mason SG. Particle motion in sheared suspensions. XIX. Viscoelastic media. *Trans Soc Rheol*. 1966;10:571–592.
35. Jossic L, Magnin A. Structuring under flow of suspensions in gel. *AIChE J*. 2004;50:2691–2696.
36. Jossic L, Magnin A. Structuring of gelled suspensions flowing through a sudden three-dimensional expansion. *J Non-Newtonian Fluid Mech*. 2005;127:201–212.

Appendix

The analytical expression of the velocity profile of a Herschel-Bulkley fluid, Eq. 1, flowing in a cylindrical pipe in steady conditions is given by:

$$\begin{cases} \frac{u(r)}{u} = \frac{3n+1}{n+1}\frac{(1-a)^{1+\frac{1}{n}} - \left(\frac{r}{R}-a\right)^{1+\frac{1}{n}}}{F(a,n)} & \text{pour } 1 \le \frac{r}{r_s} \le \frac{R}{r_s} \\ \frac{u(r_s)}{u} = \frac{3n+1}{n+1}\frac{(1-a)^{1+\frac{1}{n}}}{F(a,n)} = \frac{U_{\max}}{u} & \text{pour } 0 \le \frac{r}{r_s} \le 1 \end{cases} \quad \text{(A1)}$$

$a = \frac{\tau_0}{\tau_w} = \frac{r}{r_s}$ is the ratio of the yield stress of the fluid to stress at the wall τ_w. u designates the average velocity of the flow. The velocity of the plug zone is the maximum velocity of the velocity profile $U_{\max}$. In the case of a Herschel-Bulkley fluid:

$$F(a,n) = (1-a)^{\frac{1}{n}} \left(1 - \frac{a}{2n+1} - \frac{2n}{(n+1)(2n+1)}a^2 - \frac{2n^2}{(n+1)(2n+1)}a^3\right).$$

Manuscript received Jun. 4, 2008, and revision received Jan. 8, 2009.